Cavitation-Induced Reactions in High-Pressure Carbon Dioxide

M. W. A. Kuijpers, D. van Eck, M. F. Kemmere, J. T. F. Keurentjes*

The feasibility of ultrasound-induced in situ radical formation in liquid carbon dioxide was demonstrated. The required threshold pressure for cavitation could be exceeded at a relatively low acoustic intensity, as the high vapor pressure of CO_2 counteracts the hydrostatic pressure. With the use of a dynamic bubble model, the formation of hot spots upon bubble collapse was predicted. Cavitation-induced radical formation was used for the polymerization of methyl methacrylate in CO_2, yielding high-molecular-weight polymers. These results show that sonochemical reactions can be performed in dense-phase fluids, which allows the environmentally benign CO_2 to replace conventional organic solvents in many reaction systems.

Sonochemistry comprises all of the chemical effects that are induced by ultrasound, including the formation of radicals and the enhancement of reaction rates at ambient temperatures (*1*, *2*). The chemical effects of ultrasound are caused by cavitation: the collapse of microscopic bubbles in a liquid (*3*, *4*), a phenomenon that does not occur in boiling liquids. Cavities are generated when the "negative" pressure during the rarefaction phase of the sound wave is sufficiently large to disrupt the liquid. In water, the implosions of these cavities generate temperatures up to 5000 K and pressures up to 200 bar, because of the compression of the gas phase inside the cavity (*5*, *6*). These conditions lead to the formation of excited states, bond breakage, and the generation of radicals. As compared to the use of initiators or catalysts, cavitation-induced radical reactions allow for clean and safe operation, because no separation is required afterward and the formation of radicals can be controlled externally. On the other hand, electrical energy is required to generate cavitation.

Dense-phase fluids (with a strong emphasis on CO_2) are expected to provide a powerful means for the development of processes based on green chemistry (*7*, *8*). To generate sufficient solvent power in dense-phase fluids, high densities and hence high pressures are required. In ordinary solvents, cavitation does not occur at elevated pressures (*9*). As a result, sonochemical studies have been limited to atmospheric conditions. The use of dense-phase fluids in sonochemical reactions could open up the use of pressure as a process variable to control solubility during ultrasound-induced reactions. As an example, in polymerizations, high-pressure CO_2 will act

Process Development Group, Eindhoven University of Technology, Post Office Box 513, 5600 MB Eindhoven, Netherlands.

*To whom correspondence should be addressed. E-mail: j.t.f.keurentjes@tue.nl

as an antisolvent (*10*) and will precipitate the polymer, thus enabling a viscosity reduction that would lead to high conversions.

To initiate the growth of a cavitation bubble, an acoustic pressure above the so-called Blake threshold pressure has to be applied (*11*, *12*). During pressurization of a liquid, the Blake threshold pressure increases, which implies that higher acoustic pressures are needed to produce cavitations. The maximum acoustic pressure P_A depends on the intensity provided by the ultrasonic device (I_{US}), the density of the liquid (ρ), and the velocity of sound (c) $P_A = \sqrt{2 \times \rho \times c \times I_{US}}$. Because the velocity of sound is a function of the compressibility of the medium (*13*), the attainable acoustic pressure for a given ultrasound intensity is a function of pressure and temperature. Unlike ordinary liquids, the high vapor pressure of a dense-phase fluid (which is a gas at ambient conditions) allows cavitation to occur. As a result, the Blake threshold is reduced, which enables cavitation in liquid CO_2 at higher pressures. Figure 1 shows the calculated Blake threshold pressure for CO_2 and water at 58.2 bar. At 58.2 bar and 293 K, the Blake threshold pressure of liquid CO_2 equals the threshold pressure in water at 1 bar and 293 K. For water at 58.2 bar, a very high acoustic pressure is required to create cavitation. The threshold pressure in water is determined only by the static pressure and the surface tension of the liquid, because of its low vapor pressure. Because the vapor pressure does not change significantly with increasing temperature, the threshold pressure of water is approximately constant. Because CO_2 condenses at a substantially higher pressure, its vapor pressure has a substantial influence. Liquid CO_2 has a relatively low surface tension σ [at 293 K and 57.2 bar, σ equals 3.3×10^{-3} N/m (*13*)]. This leads to a contribution of the Laplace pressure ($2\sigma/R_0$) to the Blake threshold pressure of only 0.0066 bar at a bubble radius R_0 of 10^{-5} m, whereas the vapor pressure contribution equals 57.2 bar.

The occurrence of cavitation in high-pressure CO_2 has been shown at 75 bar and 283 K, at which CO_2 is in the liquid state, although above its critical pressure. It is important to stay below the critical point of the mixture, because above the critical point no phase boundaries exist, hence prohibiting cavitation. At an acoustic intensity below the Blake threshold pressure (25 W/cm²), the liquid remains transparent (Fig. 2A), whereas at an ultrasound intensity of 125 W/cm², cavitation occurs (Fig. 2B). Assuming a sound velocity of 800 m/s (*13*), the measured threshold intensity of 125 W/cm² corresponds with an acoustic pressure of 12.5 bar, which is below the calculated Blake threshold pressure of 30 bar. Because of the inhomogeneous temperature distribution close to the probe, however, a lower threshold pressure is expected because the threshold pressure strongly decreases at higher temperatures.

A dynamic model is required to describe the motion of the bubble and to calculate the temperature and pressure at bubble collapse (*14*). We used the Kyuchi-Yasui model (*15*, *16*), which is based on the Rayleigh-Plesset equation combined with mass and energy balances over the bubble, and we assumed that evaporation and condensation at the bubble wall are in equilibrium. The variation of the bubble radius with time is shown in Fig. 3. No bubble formation or growth occurs in water at elevated pres-
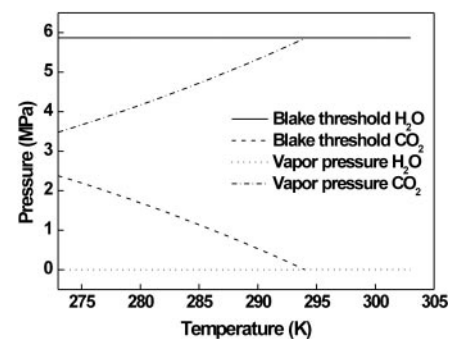

Fig. 1. Calculated Blake threshold pressure and vapor pressure for water and CO_2 at 58.2 bar. The Blake threshold pressure is calculated as

$$P_B = P_0 - P_v + \frac{4}{3}\sigma \times$$

$$\sqrt{\frac{2}{3} \times \frac{\sigma}{\left(P_0 + 2 \times \frac{\sigma}{R_0} - P_v\right) \times R_0^3}}$$

This equation assumes that the external pressure P_o, the vapor pressure P_v, the surface tension σ, and the equilibrium radius of the bubble R_0 determine the required negative pressure in the liquid to start the explosive growth of a cavity. Using $P_{v,water} = 0.023$ bar, $\sigma_{water} = 72 \times 10^{-3}$ N/m, $P_{v,CO_2} = 57.2$ bar, $\sigma_{CO_2} = 3.3 \times 10^{-3}$ N/m, and $R_o = 10^{-5}$ m, the Blake threshold pressure equals 1 bar for water at atmospheric conditions, so that in CO_2 a hydrostatic pressure of 58.2 bar is required for a threshold pressure of 1 bar.

sures. The maximum bubble radius before collapse is on the same order of magnitude for water at atmospheric conditions and in liquid CO_2 at high pressure. The calculated maximum attainable temperatures are 722 K for water (at 1 bar) and 585 K for liquid CO_2 at 58.2 bar.

To show that bubble collapse in liquid CO_2 is sufficiently strong to induce radical formation, measurements were done in CO_2-methyl methacrylate (MMA) systems at high pressure.

Fig. 2. Ultrasound-induced cavitation in liquid CO_2 at 283 K and 75 bar. The experiments were performed in a high-pressure cell of 175 ml provided with quartz windows. The tip of the ultrasound horn is located at the top and provides 20-kHz ultrasound with an intensity of 25 W/cm² (**A**) and 125 W/cm² (**B**). In (A), no cavitation occurs and the liquid remains transparent, whereas in (B) cavitation does occur, made visible by the presence of dispersed gas bubbles underneath the ultrasound horn. Additionally, the cavitation threshold can simply be determined by ear.

Fig. 3. Calculated radius of a cavitation bubble as a function of time in water and high-pressure CO_2 at 293 K. Initially, a small cavity with a radius of 10^{-5} m is present, which consists of argon and the corresponding vapor of the liquid phase. In the calculations, an ultrasound wave with an acoustic pressure of 10 bar and a frequency of 20 kHz is imposed on this bubble.
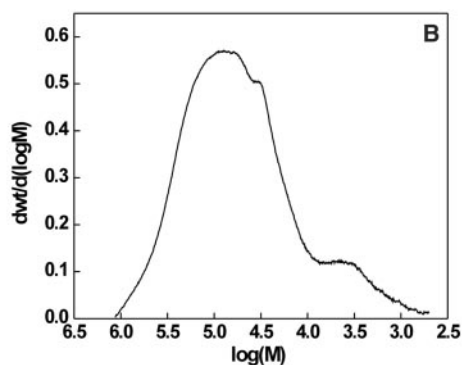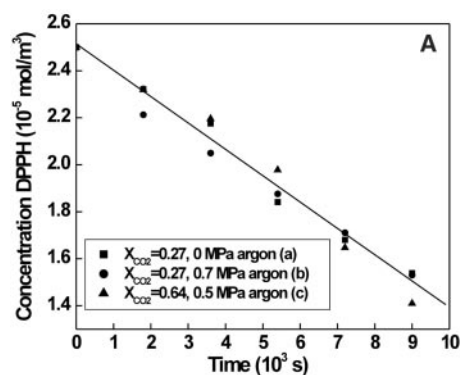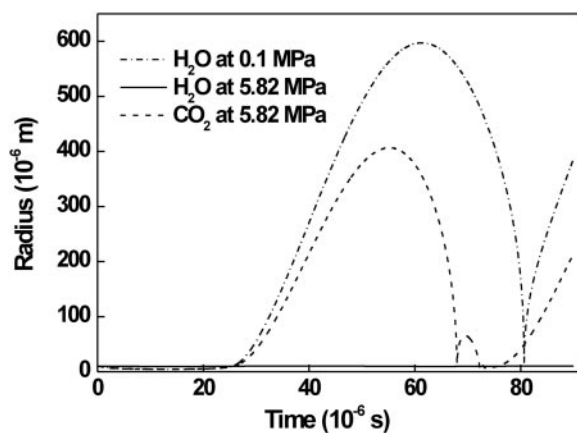
Fig. 4. (**A**) Cavitation-induced radical formation in liquid CO_2. Displayed is the concentration of the radical scavenger 1,1-diphenyl-2-picrylhydrazyl (DPPH) in time as determined by ultraviolet-visible spectroscopy analysis at 520 nm (*18*). A 175-ml high-pressure vessel was filled with MMA, which was distilled before use to remove the hydroquinone inhibitor. Argon was bubbled through the liquid, and CO_2 was added to bring the total liquid volume to 150 ml. The measurements were performed at 293 K for two CO_2:MMA ratios: 0.27:0.73 mol:mol (a and b) and 0.64:0.36 mol:mol (c), leading to pressures of 12 and 30 bar, respectively. Additionally, 7- and 5-bar argon was added for systems b and c, respectively. Subsequently, the ultrasound probe (1.24 cm²) was switched on with a frequency of 20 kHz and an intensity of 118 W/cm² (a and b). In (c), a limiting intensity of 72 W/cm² was observed. (**B**) Molecular weight distribution of the polymer obtained from the cavitation-induced polymerization of MMA after 2 hours of sonication. The experiments were performed at a molar CO_2:MMA ratio of 0.27:0.73 at 293 K. The polymer was characterized via gel permeation chromatography, which was calibrated against polystyrene standards.
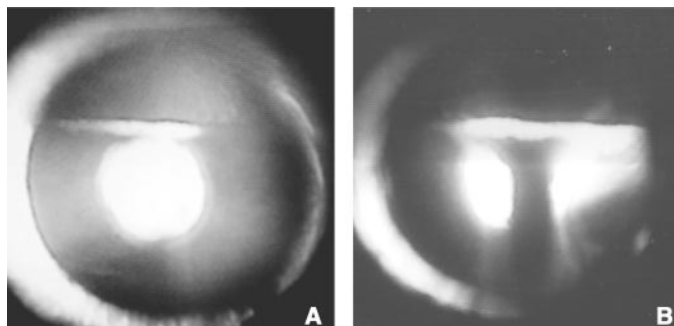
Mixing MMA with CO_2 will increase the Blake threshold pressure, so that the system will behave more like an ordinary liquid (*17*). Using the reaction calorimetry technique during ultrasound application as described in our earlier work (*18*), we found that the threshold intensity for CO_2-MMA mixtures at 293 K was 23 and 68 W/cm² for CO_2 mole fractions of 0.27 and 0.64, respectively. Although both systems are near their boiling points, the CO_2-MMA system with a high mole fraction of CO_2 requires an additional argon head pressure to avoid boiling and to allow for cavitation.

Radical formation has been measured in CO_2-MMA systems using a radical scavenger (Fig. 4A). From these results, a radical formation rate of 1.5×10^{14} s^{-1} is determined, for which no noticeable difference between the three systems is found. Additionally, polymerization experiments have been performed in the same CO_2-MMA system without the radical scavenger. In Fig. 4B, the molecular weight distribution of the formed poly (methyl methacrylate) (PMMA) is given, which shows that high-molecular-weight material is formed with a weight-averaged and number-averaged molecular weight of 100,000 and 21,000, respectively, leading to a polydispersity of about 4.9. In pure MMA, no cavitation occurs at this pressure and ultrasound intensity and hence no polymerization was observed. In ultrasound-induced bulk polymerizations at ambient pressures, a strong viscosity increase is observed, which hinders cavitation, and hence radical formation, which limits the conversion to low values (*2*). Because high-pressure CO_2 acts as an antisolvent, the polymer will precipitate from the CO_2-monomer phase, so that even at high conversions a low solvent viscosity and a high radical formation rate can be maintained.

Because cavitation can also cause chain scission, the attained molecular weight can be limited by this effect (*2*). To allow for chain scission, the polymer needs to be in solution and has to be above a certain molecular weight to experience sufficient strain on the polymer chain. Depending on the cavitation intensity and the viscosity of the system, an upper limit for the molecular weight of approximately 30,000 g/mol can be expected as a result of polymer scission. The solubility of PMMA in the system is strongly dependent on the CO_2:MMA ratio: At a CO_2:MMA ratio of 0.71:0.29, the solubility of PMMA with a number-averaged molecular weight of 46,400 g/mol is approximately 5% (*19*). Increasing the CO_2:MMA ratio, however, results in a sharp decrease in solubility. This would provide an additional means to control the molecular weight of the polymer and to obtain multimodal molecular weight distributions.

These experiments demonstrate the feasibil-

ity of ultrasound-induced in situ radical formation in liquid CO_2, thereby substantially broadening the application potential for sonochemistry as it allows for the use of environmentally benign CO_2 to replace conventional organic solvents in many reaction systems.

References
1. L. H. Thompson, L. K. Doraiswamy, *Ind. Eng. Chem. Res.* **38**, 1215 (1999).
2. G. J. Price, *Ultrason. Sonochem.* **3**, S229 (1996).
3. K. S. Suslick, *Science* **247**, 1439 (1990).
4. Y. T. Didenko, K. S. Suslick, *Nature* **418**, 394 (2002).
5. K. S. Suslick, *Sci. Am.* **260**, 80 (February 1989).
6. J.-L. Luche, *Synthetic Organic Sonochemistry* (Plenum, New York, 1998).
7. P. G. Jessop, W. Leitner, Eds., *Chemical Synthesis Using Supercritical Fluids* (Wiley-VCH, Weinheim, Germany, 1999).
8. M. A. Abraham, L. Moens, Eds., *Clean Solvents*, *Alternative Media for Chemical Reactions and Processing*, ACS Symposium Series 819 (American Chemical Society, Washington, DC, 2002).
9. J. Berlan, F. Trabelsi, H. Delmas, A. M. Wilhelm, J. F. Petrignani, *Ultrason. Sonochem.* **1**, S97 (1994).
10. K. A. Shaffer, J. M. DeSimone, *Trends Polym. Sci.* **3**, 146 (1995).
11. T. J. Leighton, *The Acoustic Bubble* (Academic Press, London, 1994).
12. S. Hilgenfeldt, P. M. Brenner, S. Grossmann, D. Lohse, *J. Fluid Mech.* **365**, 171 (1998).
13. D. P. Singh, M. Lal, B. Singh, *Acoust. Lett.* **15**, 235 (1992).
14. J. P. Lorimer, T. J. Mason, *Chem. Soc. Rev.* **16**, 239 (1987).
15. K. Yasui, *J. Acoust. Soc. Am.* **98**, 2772 (1995).
16. _____, *Ultrasonics* **36**, 575 (1998).
17. D. L. Goldfarb, H. R. Corti, F. Marken, G. J. Compton, *J. Phys. Chem. A.* **102**, 8888 (1998).
18. M. W. A. Kuijpers, M. F. Kemmere, J. T. F. Keurentjes, *Ultrasonics* **40**, 675 (2002).
19. M. Lora, M. A. McHugh, *Fluid Phase Equilibria* **157**, 285 (1999).

Closed-Shell Molecules That Ionize More Readily Than Cesium

F. Albert Cotton,[1]* Nadine E. Gruhn,[2] Jiande Gu,[3]*
Penglin Huang,[1] Dennis L. Lichtenberger,[2]* Carlos A. Murillo,[1]*
Laura O. Van Dorn,[2] Chad C. Wilkinson[1]

We report a class of molecules with extremely low ionization enthalpies, one member of which has been determined to have a gas-phase ionization energy (onset, 3.51 electron volts) lower than that of the cesium atom (which has the lowest gas-phase ionization energy of the elements) or of any other known closed-shell molecule or neutral transient species reported. The molecules are dimetal complexes with the general formula $M_2(hpp)_4$ (where M is Cr, Mo, or W, and hpp is the anion of 1,3,4,6,7,8-hexahydro-2*H*-pyrimido[1,2-*a*]pyrimidine), structurally characterized in the solid state, spectroscopically characterized in the gas phase, and modeled with theoretical computations. The low-energy ionization of each molecule corresponds to the removal of an electron from the delta bonding orbital of the quadruple metal-metal bond, and a strong interaction of this orbital with a filled orbital on the hpp ligands largely accounts for the low ionization energies.

The phenomena of oxidation (electron loss) and reduction (electron gain) are fundamental to chemistry. Even when these processes do not occur as such, more complex chemical processes and properties, such as ionic and covalent bond formation and acid-base behavior, can be understood by analyzing them as a sum of oxidation and reduction steps. Tables of oxidation enthalpies, electron affinities, and electrode (redox) potentials are essential to understanding and teaching chemistry.

[1]Department of Chemistry and Laboratory for Molecular Structure and Bonding, Texas A&M University, Post Office Box 30012, College Station, TX 77842–3012, USA. [2]Department of Chemistry and Laboratory for Gas-Phase Electron Spectroscopy, The University of Arizona, Tucson, AZ 85721, USA. [3]Drug Design and Discovery Center, State Key Laboratory of Drug Research, Shanghai Institute of Materia Medica, Shanghai Institutes for Biological Sciences, Chinese Academy of Sciences, Shanghai 200031, China.

*To whom correspondence should be addressed. E-mail: cotton@tamu.edu (F.A.C.); jiandegush@go.com (J.G.); dlichten@email.arizona.edu (D.L.L.); murillo@tamu.edu (C.A.M.)

Molecules that are thermodynamically stable under normal conditions typically have closed shells of valence electrons and ionization enthalpies of at least 7 eV. The closed-shell molecule with the lowest ionization enthalpy (5.17 eV, vertical) is [(η^5-$C_5H_4{}^iPr$)MoSe]$_4$ (*1*). In general, values below 5 eV are observed only for molecules or atoms with at least one electron alone in an outer orbital, and even then additional conditions must apply. Typical examples are the alkali metal atoms, which are well known as powerful reducing agents (*2*). Lithium and sodium atoms have ionization enthalpies above 5 eV (5.39 and 5.14 eV, respectively), and only the heavier alkali metals have ionization enthalpies less than 5 eV, with the cesium atom having the lowest of all the elements at 3.89 eV (*3*). We report here measurements and modeling of a class of closed-shell molecules with extremely low ionization energies (IEs). One member of this class ionized at significantly lower energy than cesium atoms and far lower than any

other molecules that have been chemically prepared up to this time (*4*–*6*).

We are currently studying the remarkable ability of the hpp ligand (the anion of 1,3,4,6,7,8-hexahydro-2*H*-pyrimido[1,2-*a*]pyrimidine) to cause large negative shifts in the oxidation potentials of paddlewheel complexes of the $M_2(hpp)_4X_n$ ($n = 0, 1, 2$) type, as indicated in electrochemical studies. Recently we reported that the $Mo_2(hpp)_4$ molecule (*7*) (Fig. 1) is so easily oxidized that a chlorinated solvent such as CH_2Cl_2 oxidizes it essentially quantitatively to $Mo_2(hpp)_4Cl$ (*8*). In order to take the $Mo_2(hpp)_4Cl$ molecule to $Mo_2(hpp)_4Cl_2$ or others containing the $[Mo_2(hpp)_4]^{2+}$ unit, an additional (and stronger) oxidizing agent, such as O_2 or Ag^+, is required, but even this oxidation is facile and the product remarkably stable as compared with the reactivity of all other paddlewheel complexes of the Mo_2^{4+} core (*9*).

There are a number of other cases in which $M_2(hpp)_4Cl_2$ molecules have been found to be much more accessible than analogous paddlewheel molecules in which
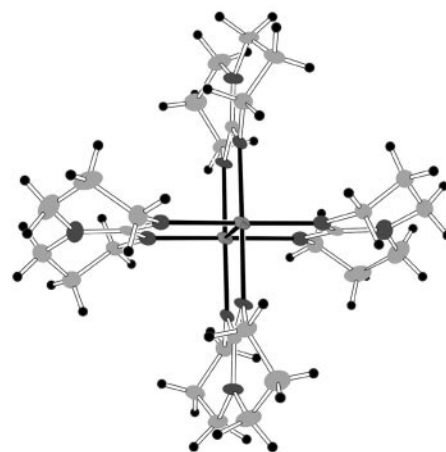

Fig. 1. A thermal ellipsoid drawing of the quadruply bonded $M_2(hpp)_4$ molecules (M = Mo and W) based on X-ray crystallography (*7*, *8*, *13*). The nonplanarity of the ligands is clearly shown. Distances: Mo–Mo = 2.067(1) Å; W–W = 2.162(1) Å; Mo^4N(av) = 2.157[7] Å; W–N(av) = 2.128[5] Å.